Exchange-coupled FePt nanoparticle assembly

Hao Zeng[a] and Shouheng Sun
IBM T. J. Watson Research Center, Yorktown Heights, New York 10598

T. S. Vedantam and J. P. Liu
Institute for Micromanufacturing, Louisiana Tech University, Ruston, Louisiana 71272

Z.-R. Dai and Z.-L. Wang
School of Materials Science and Engineering, Georgia Institute of Technology, Atlanta, Georgia 30332

(Received 21 November 2001; accepted for publication 7 February 2002)

We have produced exchange-coupled FePt nanoparticle assemblies by chemical synthesis and subsequent thermal annealing. As the interparticle distances decrease by tuning the annealing conditions, interparticle interactions change from dipolar type to exchange type, and the magnetization reversal mechanism switches from rotation controlled to domain-nucleation controlled. With increasing annealing temperature, the coercivity first increases due to improved chemical ordering, and then drops significantly, resulting from excessive interparticle exchange coupling. For the samples exhibiting exchange coupling, both the remanence ratio and coercive squareness increase. © *2002 American Institute of Physics.* [DOI: 10.1063/1.1467976]

High-performance permanent magnets for energy-related applications require a large energy product $(BH)_{\max}$. A permanent magnet with a large $(BH)_{\max}$ value should exhibit both high remanent magnetization M_r and large coercivity H_c. Both parameters are determined not only by intrinsic properties such as the magnetocrystalline anisotropy K_u and saturation magnetization M_s, but also by structural parameters such as grain sizes and alignment of the granular materials. Tremendous effort has been devoted in the last century to improving magnetic properties of permanent magnets,[1] however, it is recently realized that nanostructured magnetic materials have the potential for a very high energy product.[2,3]

$L1_0$-ordered FePt alloys have high M_s ($\sim$1100 emu/cm^3) and large K_u ($>5\times10^7$ erg/cm^3) and, therefore, are attractive as permanent magnetic materials. In the past decades, the hard-magnetic properties of FePt alloys have been studied extensively,[4,5] however, little has been done on nanostructured FePt systems. Recent progress in the synthesis of FePt nanoparticles[6] makes it possible to utilize nanostructured FePt for potential permanent magnet applications, because chemical methods have the advantages of highly controllable particle sizes and morphologies. Here, we report detailed magnetic studies on FePt nanoparticle assemblies produced by solution-phase synthesis and self-assembly, followed by thermal treatment. We find that the thermal treatment controls not only the formation of the high anisotropy L_{10} FePt phase but also the interparticle exchange of the nanoparticles.

The high-temperature solution phase decomposition of $Fe(CO)_5$ and reduction of $Pt(acac)_2$ produces monodispersed FePt nanoparticles with the composition controlled by the molar ratio of $Fe(CO)_5$ and $Pt(acac)_2$.[6,7] Deposition of nanoparticle dispersion on a solid substrate and controlling solvent evaporation lead to FePt nanoparticle assemblies. The structural properties were characterized by transmission electron microscopy and x-ray diffractometry (XRD), and the magnetic properties were measured by a superconducting quantum interference device magnetometer. As-synthesized particles possess a disordered fcc structure, which are superparamagnetic at room temperature due to small sizes and low anisotropy. Thermal annealing results in a phase transformation from the disordered fcc to ordered fct structure above 500 °C.[6] All samples were annealed at temperatures between 500 and 800 °C for 1 h, in a flow of gas mixture of Ar $+H_2$ (5%). No preferential orientation of the particles is observed from either XRD or electron diffractions. Previous works have indicated that for FePt with various compositions $Fe_{54\text{-}58}Pt_{46\text{-}42}$ shows the largest coercivities after annealing.[7] Here, we specifically choose Fe-rich $Fe_{58}Pt_{42}$, which may yield both large H_c and high magnetization.

Annealing at higher temperatures leads to the evaporation/decomposition of the organic surfactant around each particle and the decrease of interparticle distances. Tuning of the interparticle distances is realized by carefully controlling the self-assembly and annealing conditions, in an attempt to optimize the nanostructures for high $(BH)_{\max}$. *In situ* transmission electron microscopy (TEM) studies on the annealed nanoparticles show no significant aggregation at annealing temperatures T_a below 600 °C.[8] As seen from Fig. 1(a), for a sample annealed at 530 °C, neither the interparticle distances nor the ordering shows much change compared to as-deposited samples. At 600 °C or slightly above, particles start to aggregate [Fig. 1(b)]. However, detailed high-resolution TEM (HRTEM) studies [see the inset of Fig. 1(b)] show that the coalesced particles do not form single-crystal agglomerates; instead, two originally separated particles form a twin structure with the grain boundaries being easily visible. There is no evidence of carbon residue present at the grain boundaries, as opposed to previous results on samples annealed at low temperatures under N_2.[6] It is expected that even higher temperatures will eventually lead to significant agglomerations and the formation of continuous films.

Chemically ordered fct FePt nanoparticles may show

[a]Electronic mail: haozeng@us.ibm.com

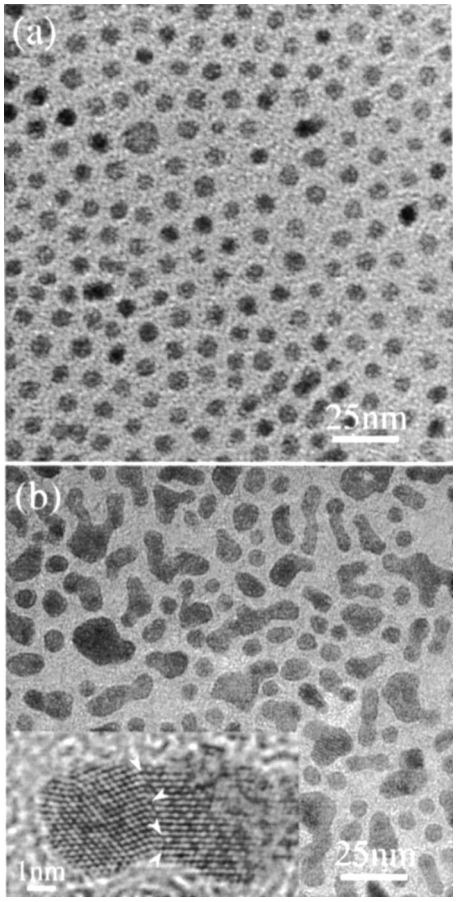

FIG. 1. TEM image of 4 nm FePt nanoparticle assemblies after annealing to (a) 530 °C and (b) 600 °C, the inset is the HRTEM of two aggregated FePt particles.

large coercivity originating from their large K_u.[4] The degree of ordering depends strongly on the annealing temperatures. Figure 2 shows the room-temperature H_c as a function of T_a, with the annealing time fixed as 1 h. H_c first increases rapidly as T_a increases from 500 to 600 °C, and then decreases dramatically with further increasing T_a. A peak value of $H_c \sim 20$ kOe appears at 600 °C. The rising of H_c with increasing T_a below 600 °C is mainly due to the improvement of the chemical ordering of the FePt particles, leading to the increase of K_u. The decrease of H_c above 600 °C is very interesting and will be discussed below.

The reduction of interparticle distances with increasing

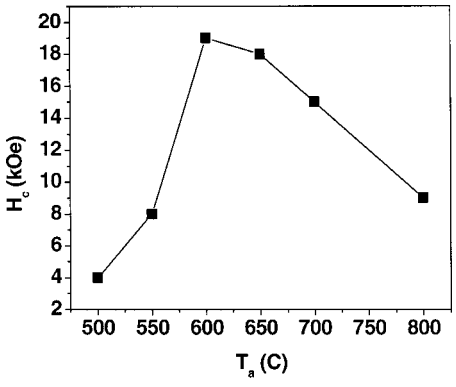

FIG. 2. Coercivity H_c as a function of the annealing temperature T_a, with the annealing time fixed to be 1 h.

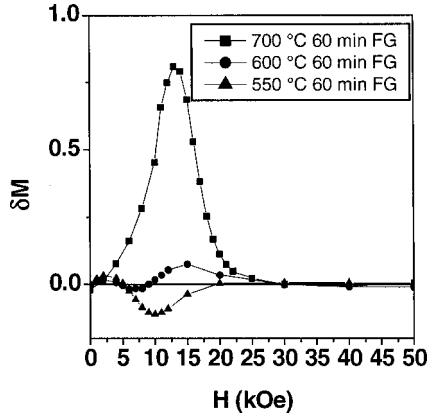

FIG. 3. δM curves for samples annealed at 550, 600, and 700 °C, respectively.

T_a results in dramatic changes in interparticle interactions. Figure 3 shows δM curves for $T_a = 550$, 600, and 700 °C, respectively. δM is defined as $M_d - (1 - 2M_r)$, where M_d is the reduced dc demagnetization remanence curve, and M_r the reduced isothermal remanence curve. The δM parameter has been used to characterize interparticle interactions in particulate systems.[9] It can be seen from Fig. 3 that for $T_a = 550$ °C, δM shows a negative peak, indicating that the predominant interparticle interactions are dipolar. This is consistent with the TEM observation that all of the particles are well separated at this annealing temperature. For $T_a = 700$ °C, however, the δM curve shows a large positive peak, indicating strong exchange coupling. δM shows a small positive peak for $T_a = 600$ °C, where particles just start to touch each other and common grain boundaries are observed [Fig. 1(b)].

The initial magnetization curves and hysteresis loops are shown in Fig. 4. It is seen that for the sample annealed at 550 °C, which consists of well-separated particles, the remanence ratio is 0.55. This is close to the value of 0.5 predicted for randomly oriented, noninteracting Stoner–Wohlfarth particles. The random orientation together with weak interparticle interactions leads to a broad switching field distribution (SFD). Additionally, the anisotropy distribution may also contribute to the broadening of the SFD. In a previous work, physically monodispersed cobalt nanoparticle assemblies (3–5 nm) also show wider than expected anisotropy distribution due to the internal structure, shape, and surface atom effects.[10] For $T_a = 600$ °C, the hysteresis loops show a much higher remanence ratio, and the slope near coercivity is much steeper. This cooperative switching behavior again infers that the dominant interparticle interaction is exchange coupling.[11]

The degree of particle aggregation and changes in interparticle interactions also result in different magnetization reversal behaviors. As seen in Fig. 4, for T_a at or below 600 °C, the initial magnetization curves resemble that for magnetization rotation of individual particles,[12] which is consistent with weak interparticle interactions. For $T_a = 800$ °C, however, the initial curve rises steeply at small fields and tends to saturate at lower fields, as compared to the previous samples. This suggests that for the samples annealed at higher temperatures, the magnetization reversal mechanism is controlled mainly by domain nucleation pro-

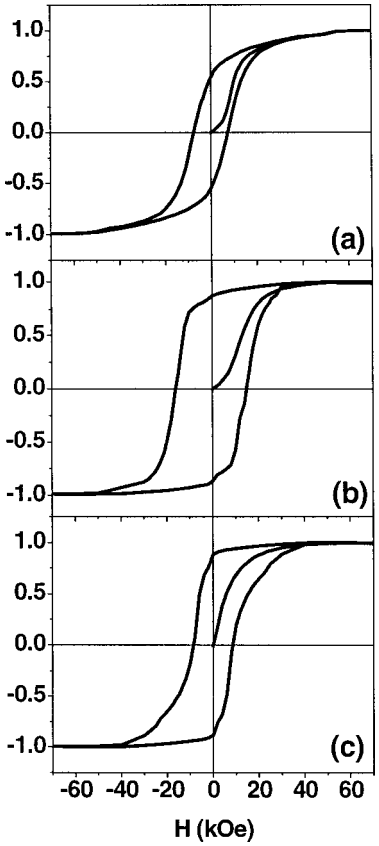

FIG. 4. Initial magnetization curves and hysteresis loops for samples annealed at (a) 550 °C, (b) 600 °C, and (c) 800 °C, respectively.

cesses. The particle agglomeration leads to the formation of polycrystalline films, which gives more chances for nucleation of reversed domains. The decrease of H_c at T_a above 600 °C may partly be attributed to the change in reversal mechanisms. Another important factor in reducing H_c is the random anisotropy effects (RAE).[13] As the particle radius becomes smaller than the domain-wall width parameter $\delta_w = (A/K_1)^{1/2}$, which is about 2–4 nm depending on the parameters chosen, the effective anisotropy is an average over several grains, and reduced in magnitude.[14] For the FePt nanoparticles in this study, the particle radius is comparable to δ_w, and the extent to which RAE affects the macroscopic anisotropy is very sensitive to these parameters. Detailed work on quantifying RAE is underway.

Temperature-dependent coercivity $H_c(T)$ has been measured for samples annealed at 550 and 800 °C, respectively (Fig. 5). For $T_a = 550$ °C, H_c drops significantly with increasing T, this is mainly due to the strong thermal effects in the nanoparticles. A fit using Sharrock's formula[15] gives $H_0 = 20$ kOe, where H_0 is the zero-temperature coercivity and $K_u V = 2.5 \times 10^{-12}$ erg. Recently, it was pointed out by Chantrell that Sharrock's formula overestimates K_u for systems containing superparamegnetic particles.[16] H_0 is roughly 50% of the value expected for bulk FePt. This may be associated with partial ordering resulting in lower anisotropy, and/or incoherent magnetization reversal. HRTEM shows that the shape of these particles deviates from ideal spheres, and in many cases possesses the shape of polygons such as the truncated octahedron.[17] This may lead to curling reversal, or even a more complicated situation if inhomogeneities

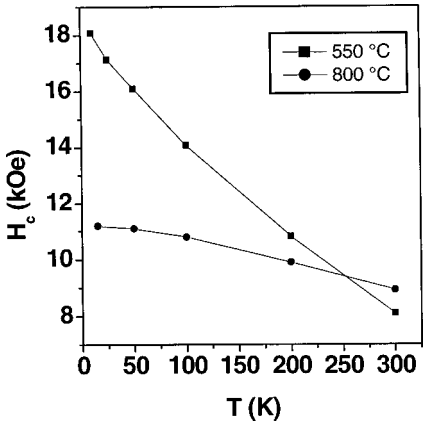

FIG. 5. Coercivity as a function of temperature for samples annealed at (a) 550 °C, and (b) 800 °C, respectively.

within the nanoparticles are present. For $T_a = 800$ °C, H_c shows much weaker temperature dependence, especially at low temperatures. This suggests that highly exchange-coupled polycrystalline films show much less thermal effects, and the temperature dependence of H_c most probably originates from the temperature dependence of K_u.

Our results show that optimal magnetic hardening is achieved in the highly chemically ordered FePt nanoparticles through proper heat treatments. In such a magnetic nanoparticle assembly, the magnetization rotation of individual particles yields high coercivity. The interparticle exchange coupling caused by moderate aggregation of particles is adequate to give a high remanence ratio and coercive squareness, which is mandatory for permanent magnet applications. However, excessive exchange coupling leads to the decrease of the coercivity.

The authors would like to thank G. Held and E. E. Fullerton for the critical reading of the manuscript and helpful discussions. This work is supported in part by U.S. DoD/DARPA through ARO under Grant No. DAAD 19-01-1-0546.

[1] K. H. J. Buschow, in *Ferromagnetic Materials*, edited by E. P. Wohlfarth and K. H. J. Buschow (Elsevier Science, Amsterdam, 1988), Vol. 4.
[2] R. Coehoorn, D. B. de Mooij, and C. de Waard, J. Magn. Magn. Mater. **80**, 101 (1989).
[3] R. Skomski and J. M. D. Coey, Phys. Rev. B **48**, 15812 (1993).
[4] K. Watanabe and H. Masumoto, J. Jpn. Inst. Met. **48**, 930 (1984).
[5] J. P. Liu, C. P. Luo, Y. Liu, and D. J. Sellmyer, Appl. Phys. Lett. **72**, 483 (1998).
[6] S. Sun, C. B. Murray, D. Weller, L. Folks, and A. Moser, Science **287**, 1989 (2000).
[7] S. Sun, E. E. Fullerton, D. Weller, and C. B. Murray, IEEE Trans. Magn. **37**, 1239 (2001).
[8] Z. R. Dai, S. Sun, and Z. L. Wang, Nano Lett. **1**, 443 (2001).
[9] P. E. Kelly, K. O'Grady, P. I. Mayo, and R. W. Chantrell, IEEE Trans. Magn. **25**, 3881 (1989).
[10] S. I. Woods, J. R. Kirtley, S. Sun, and R. H. Koch, Phys. Rev. Lett. **87**, 137205 (2001).
[11] R. Skomski and D. J. Sellmyer, J. Appl. Phys. **89**, 7263 (2001).
[12] B. D. Cullity, *Introduction to Magnetic Materials* (Addison-Wesley, Reading, MA, 1972).
[13] E. M. Chudnovski, W. M. Saslow, and R. A. Serota, Phys. Rev. B **33**, 251 (1986).
[14] G. Herzer, Mater. Sci. Eng., A **133**, 1 (1991).
[15] M. P. Sharrock, J. Appl. Phys. **76**, 6413 (1994).
[16] R. W. Chantrell, D. Weller, T. J. Klemmer, S. Sun, and E. E. Fullerton, J. Appl. Phys. **91** (in press).
[17] Z. R. Dai, Z. L. Wang, and S. Sun, Surf. Sci. (to be published).